Behaviour of carbon nanotube bundle under quasistatic and dynamic transverse compression

Behaviour of carbon nanotube bundle under quasistatic and dynamic transverse compression

L Kh Rysaeva[1], R T Murzaev[1], A A Kudreyko[2], E A Korznikova[1,3] and S V Dmitriev[1,4]

[1] Institute for Metals Superplasticity Problems of RAS, 450001, 39 Khalturin St., Ufa, Russia
[2] Department of Medical Physics and Informatics, Bashkir State Medical University, 47 Zaki Validi st., 47, 450000 Ufa, Russia
[3] Ufa State Aviation Technical University, 450077, 12 Karl Marx, Ufa, Russia
[4] Institute of Molecule and Crystal Physics, Ufa Federal Research Centre of the Russian Academy of Sciences, 71 October Avenue, 450054 Ufa, Russia

E-mail: lesya813rys@gmail.com

Abstract. Carbon nanotubes (CNTs) have a unique combination of physical and mechanical properties, which makes them attractive for a number of applications. Investigation of the mechanical response of a CNT bundle under conditions of plane strain (uniaxial and biaxial lateral compression), since it can be used as an elastic damper for vibration and shock protection. In this work, using a chain model with a reduced number of degrees of freedom, the behaviour of a CNT bundle under uniaxial lateral compression is investigated. Quasistatic loading is used to calculate the elastic constants of the bundle. Dynamic loading reveals the propagation of shock waves of two types: the faster one propagates with the speed of longitudinal sound and causes insignificant deformation of the CNT cross sections, while the second one propagates approximately three times slower and leads to the collapse of the CNTs.

1. Introduction

Carbon nanotubes (CNTs) are attracted to each other by relatively weak van der Waals forces and can create molecular crystals, also called CNT bundles [1-3]. CNT bundles can be obtained by various techniques [4,5]. They have excellent mechanical properties, since individual CNT has a very high tensile strength in the range from 11 to 63 GPa, tensile Young's modulus ranging from 1.0 to 1.3 TPa and a high strain to fracture of about 10% [6,7]. In addition, CNTs are flexible, lightweight, good thermal and electrical conductors; therefore, they can be offered for a number of applications [8, 9]. The most important mechanical applications of CNTs are high-strength ropes [2, 10], fibers [11, 12], composites with a polymer and metal matrix [12, 13], solid lubricants [14], shock protecting structures [15], etc. Computer simulation studies contribute to a better understanding of the physical and mechanical properties of CNT bundles. Transformation of a vertically aligned into a horizontally aligned CNT forest by applying pressure has been studied in [16,17]. The shell model has been used to describe an ensemble of CNTs of different morphology [18]. The applicability of the beam, plate and shell models to the analysis of the mechanical properties of nanomaterials has been analyzed in [19,20]. CNTs having diameter is above a threshold value can exist either in circular or collapsed state [21-23]. For the study of mechanical response of CNT bundles the nonlinear coarse-grained potentials has been developed [24]. In order to reduce the number of degrees of freedom considered in simulation of some sp^2-carbon nanostructures, the chain model has been developed [25]. This model was successfully applied to modeling of structure and properties of carbon nanoribbon folds and scrolls [25-29] and surface ripplocations [30]. In the works [31,32], the chain model was extended to

the study of CNTs under lateral compression in plane strain conditions. Damping properties of CNT bundle were described in [33]. Mechanical properties and phase transitions in CNT bundle under lateral compression were analyzed in [34,35]. Twisted graphene nanoribbons show enhanced resistance to axial compression [36,37]. Solitary waves [30,38] and shock waves [39] in nanomaterials have also been analyzed, although dynamic problems remain much less studied.

So far, the chain model was used for the analysis of static loading of CNT bundles [31-35], and in this work, we also consider dynamical loading (shock compression).

2. Simulation details and numerical results

2.1. Simulation setup

The CNT bundle consists from single walled CNTs of the same diameter with a zigzag orientation. The *z*-axis of the Cartesian coordinate system is directed along the axes of CNTs. The bundle cross section is parallel to the *xy*-plane. The CNT cross sections form a triangular lattice with the close packed direction aligned with the *x*-axis [see figure 1(a)]. The computational cell includes 10×12 (8×200) nanotubes for static (dynamic) problem. The boundary conditions are periodic. The CNT bundle is treated under the plain strain condition. Each CNT cross section is represented by 30 carbon atoms, and each atom represents a rigid row of atoms parallel to the CNT axis (*z*-axis). Each atom has two degrees of freedom, the *x*- and *y*-components of the displacement vector.

Quasistatic compression is performed along the *x*-axis ($\varepsilon_{xx}<0$, $\varepsilon_{yy}=0$) and dynamic loading along the y-axis ($\varepsilon_{xx}=0$, $\varepsilon_{yy}<0$). Quasistatic compression is done in a stepwise manner with the increment $\Delta\varepsilon_{xx}$=-0.005 followed by relaxation. Absolute value of the volumetric strain $|\theta|=|\varepsilon_{xx}+\varepsilon_{yy}|/2=\varepsilon_{xx}/2$ is used as the measure of quasistatic strain. Shock compression loading is performed by moving the upper row of CNTs down and fixing positions of atoms in the bottom row of CNTs. The upper row moves with the velocity V=-1000m/s, which is the speed of a bullet.

2.2. Quasistatic loading

We firstly present the simulation results for quasistatic loading. In figure 1 CNT structure at different levels of uniaxial compression along the *x*-axis are shown: (a) $|\theta|=0$, (b) $|\theta|=0.08$ and (c) $|\theta|=0.3$. In (b) the undeformed structure has translational symmetry with single CNT in a primitive translational cell. Uniaxial compression results in elliptization of CNT cross sections keeping the crystallinity of the structure. At $|\theta|=0.07$ a phase transition with period doubling in two directions occurs. It can be seen that in (b) the CNT bundle has translational symmetry with four CNTs in a primitive translational cell. At $|\theta|=0.12$ another phase transition takes place when CNTs start to collapse. With increasing compressive strain the fraction of collapsed CNTs gradually increases and in (c) at $|\theta|=0.3$ almost all CNTs are collapsed.

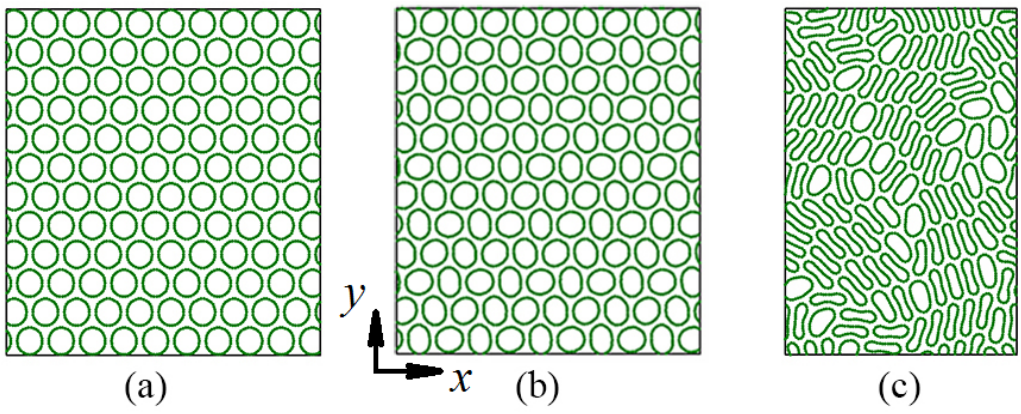

Figure 1. CNT bundle structure evolution during uniaxial compression along the *x*-axis: (a) initial state at $|\theta|=0$, (b) period doubling for the primitive translational cell at $|\theta|=0.08$ and (c) almost all CNTs are collapsed at $|\theta|=0.3$.

In figure 2(a) the stress-strain curves are presented. It can be seen that in the range $0<|\theta|<0.07$ stress components grow rapidly with strain and compressive stress σ_{xx} is greater than σ_{yy}. We do not show the shear stress because it is close to zero. At $|\theta|=0.07$ stress components show a sharp change in the slope and in the range $0.07<|\theta|<0.12$ they vary linearly with strain. At $|\theta|=0.12$ a drop of stress components takes place due to the collapse of some CNTs.

We then calculate elastic constants (Poisson's ratios ν_{xy} and ν_{yx}, Young's moduli E_{xx} and E_{xy} and shear modulus G) for the CNT bundle as the functions of volumetric strain. The Poisson's ratios are shown in figure 2(b), while the Young's moduli in figure 2(c). Interestingly, Poisson's ratios in the range $0<|\theta|<0.07$ are close to unity and they approach this value with increasing compressive strain. Even more interesting is that in the range $0.07<|\theta|<0.12$ ν_{yx} is negative and ν_{xy} remains positive with the value close to 0.3. This means that in this range of volumetric strain CNT bundle is a partial auxetic. Young's moduli and shear modulus grow linearly with compressive strain in the range $0<|\theta|<0.07$. The shear modulus exhibits a considerable increase in the range $0.07<|\theta|<0.12$, while Young's moduli a smaller in this range of strain.

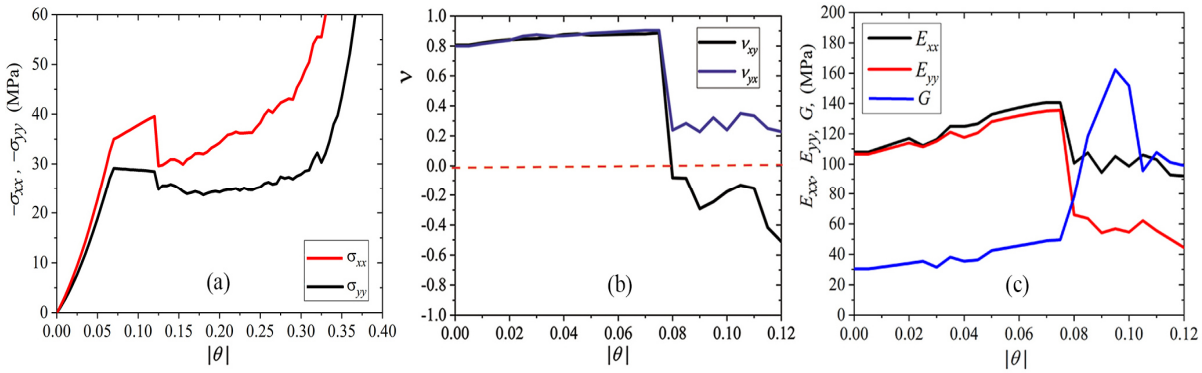

Figure 2. (a) Stress-strain curves. Change in (b) Poisson's ratios and (c) in shear modulus and Young's moduli with compressive volumetric strain.

2.3. Dynamic loading

We now turn to the presentation of the results of dynamical loading of CNT bundle, which are given in figure 3. In (a) one can see the vertical displacements of the centres of gravity of CNTs at t_1=10 ps (black line), t_2=20 ps (red line) and t_3=30 ps (blue line). Note that the horizontal rows of CNTs are numbered by the index n. In (b), as the function of n, the ellipticity of CNTs is shown as the ratio of the minimal to maximal diameters. In (c) and (d) the averaged energies of valence bonds and valence angles, respectively are shown as the functions of n. Comparison of the results shown in (a) and (b) suggests that propagation of the faster wave results in a weak elliptization of CNTs with D_{min}/D_{max}=0.9. The second slow wave leads to collapse of CNTs with D_{min}/D_{max}=0.2. As it follows from (c), energies of valence bonds are approximately same in the collapsed and non-collapsed CNTs. On the other hand, the energies of the valence angle [see in (d)], as expected, are much higher in the collapsed CNTs as compared to CNTs with small ellipticity.

3. Conclusions

Molecular dynamics simulations of quasistatic and dynamic lateral compression of CNT bundle in plane strain state were performed. Quasistatic compression along the close packed direction of the bundle (along the x-axis) has revealed that in the crystalline structural state with single CNT in the primitive translational cell Poisson's ratios are close to unity and approach this value with increasing compressive strain. It should be noted that most elastic bodies have Poisson's ratio close to 0.3, and the value of Poisson's ratio, close to unity, is extremely large. This means that the CNT bundle exhibits unusual elastic properties. When CNT bundle has crystalline structure with four CNTs in the primitive translational cell, one of the two Poisson's ratios becomes negative meaning that the bungle is a partial auxetic. Shock compression of CNT bundle in the direction normal to the close packed direction

(along the *y*-axis) has revealed propagation of two waves moving with different velocities. The faster wave caused small elliptization of CNTs, while the following slow wave causes their collapse. Results presented in this work demonstrate that elastic bodies composed of highly deformable units, such as CNT cross sections, can demonstrate unusual mechanical properties. In future works, the chain model can be extended for 2D materials other than graphene [41].

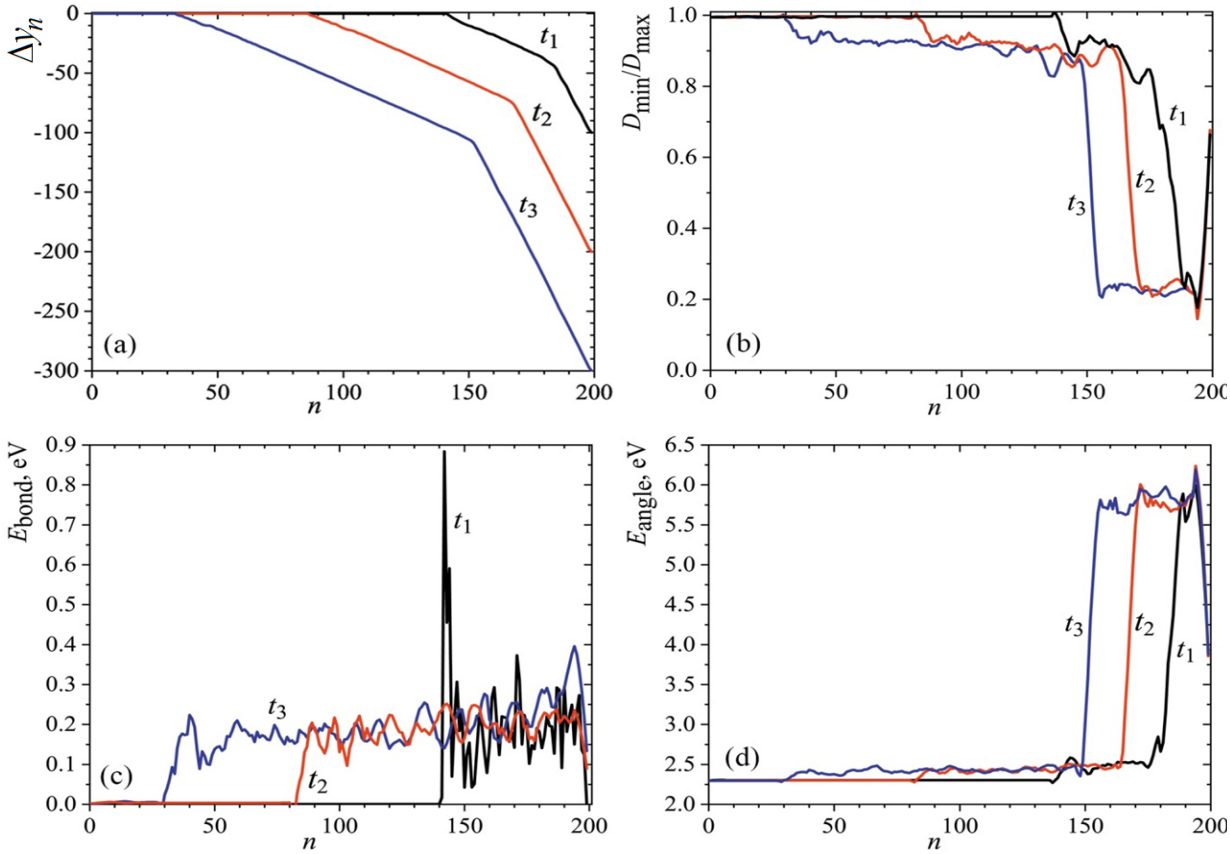

Figure 3. Displacements of the centers of mass of nanotubes under compression (a), minimal to maximal diameter ratio (b), energy valence bonds (c) and angles (d) at loading speed of 1000 m/c. t_1, t_2 and t_3 correspond to the simulation time 10 ps - black curve, 20 ps - red curve and 30 ps -blue curve.

Acknowledgments
This work was supported by the State Assignment of IMSP RAS No. AAAA-A17-117041310220-8.

References

[1] Tersoff J and Ruoff R S 1994 *Phys. Rev. Lett.* **73** 676
[2] Thess A, Lee R, Nikolaev P, Dai H, Petit P, Robert J, Xu C, Lee Y H, Kim S G, Rinzler A G, Colbert D T, Scuseria G E, Tomanek D, Fischer J E and Smalley RE 1996 *Science* **273** 483
[3] Saether E, Frankland S J V and Pipes R B 2003 *Compos. Sci. Technol.* **63** 1543
[4] Rakov E G 2013 *Russ. Chem. Rev.* **82** 538
[5] Bedewy M, Meshot E R, Guo H, Verploegen E A, Lu W and Hart A J 2009 *J. Phys. Chem.* C **113** 20576
[6] Shenderova O A, Zhirnov V V and Brenner D W 2002 *Crit. Rev. Sol. State* **27** 227-356
[7] Yu M-F 2004 *J. Eng. Mater. Technol.* **126** 271-278
[8] Truong T K, Lee Y and Suh D 2016 *Current Applied Physics* **16** 1250-1258
[9] Yao X, Hawkins S C and Falzon B G 2018 *Carbon* **136** 130-138
[10] Yu M-F, Files B S, Arepalli S and Ruoff R S 2000 *Phys. Rev. Lett.* **84** 5552-5555

[11] Bai Y, Zhang R, Ye X, Zhu Z, Xie H, Shen B, Cai D, Liu B, Zhang C, Jia Z, Zhang S, Li X and Wei F 2018 *Nature Nanotechnology* **13** 589-595
[12] Dang Z-M, Yuan J-K, Zha J-W, Zhou T, Li S-T and Hu G-H 2012 *Prog. Mater. Sci.* **57** 660
[13] Bakshi S R, Lahiri D and Agarwal A 2010 *Int. Mater. Rev.* **55** 41
[14] Reinert L, Lasserre F, Gachot C, Grützmacher P, Maclucas, Souza N, Mücklich F and Suarez S 2017 *Sci. Rep.* **7** 42873
[15] Randjbaran E, Majid D L, Zahari R, Sultan M T H and Mazlan N 2020 *Facta Universitatis Ser.: Mech. Eng.* **18** 229
[16] Wittmaack B K, Volkov A N and Zhigilei L V 2019 *Carbon* **143** 587
[17] Wittmaack B K, Volkov A N and Zhigilei L V 2018 *Compos. Sci. Technol.* **166** 66
[18] Yakobson B I, Brabec C J and Bernholc J 1996 *Phys. Rev. Lett.* **76** 2511
[19] Rafii-Tabar H, Ghavanloo E and Fazelzadeh S A 2016 *Phys. Rep.* **638** 1
[20] Harik V M 2001 *Solid State Commun.* **120** 331
[21] Impellizzeri A, Briddon P and Ewels C P 2019 *Phys. Rev.* B **100** 115410
[22] Chopra N G, Benedict L X, Crespi V H, Cohen M L, Louie S G and Zettl A 1995 *Nature* **377** 135
[23] Chang T 2008 *Phys. Rev. Lett.* **101** 175501
[24] Ji J, Zhao J and Guo W 2019 *J. Mech. Phys. Solids* **128** 79
[25] Savin A V, Korznikova E A and Dmitriev S V 2015 *Phys. Rev.* B **92** 035412
[26] Savin A V, Korznikova E A and Dmitriev S V 2015 *Phys. Solid State* **57** 2348
[27] Savin A V, Korznikova E A, Lobzenko I P, Baimova Y A and Dmitriev S V 2016 *Phys. Solid State* **58** 1278
[28] Savin A V, Korznikova E A, Dmitriev S V and Soboleva E G 2017 *Comp. Mater. Sci*. **135** 99
[29] Savin A V and Mazo M A 2019 *Adv. Struct. Mat*. **94** 241
[30] Savin A V, Korznikova E A and Dmitriev S V 2019 *Phys. Rev.* B **99** 235411
[31] Korznikova E A, Rysaeva L K, Savin A V, Soboleva E G, Ekomasov E G, Ilgamov M A and Dmitriev S V 2019 *Materials* **12** 3951
[32] Abdullina D U, Korznikova E A, Dubinko V I, Laptev D V, Kudreyko A A, Soboleva EG, Dmitriev S V and Zhou K 2020 *Computation* **8** 27
[33] Rysaeva L K, Korznikova E A, Murzaev R T, Abdullina D U, Kudreyko A A, Baimova J A, Lisovenko D S and Dmitriev S V 2020 *Facta Universitatis Ser.: Mech. Eng.* **18** 1
[34] Abdullina D U, Kudreyko A A, Korznikova E A, Shepelev I A and Dmitriev S V 2020 *Progress in Biomedical Optics and Imaging - Proceedings of SPIE* **11459** 1145911
[35] Babicheva R I, Dmitriev S V, Korznikova E A and Zhou K 2019 *J. Exp. Theor. Phys.* **129** 66
[36] Savin A V, Korznikova E A, Krivtsov A M and Dmitriev S V 2020 *Eur. J. Mech.* A. **80** 103920
[37] Savin A V, Korznikova E A and Dmitriev S V 2019 *Mech. Mater.* **137** 103123
[38] Korznikova E A and Dmitriev S V 2014 *J. Phys.* D **47** 34
[39] Shepelev I A, Chetverikov A P, Dmitriev S V and Korznikova E A 2020 *Comp. Mater. Sci*. **177** 109549
[40] Hosseini-Hashemi S, Sepahi-Boroujeni A and Sepahi-Boroujeni S 2018 *Appl. Surf. Sci.* **437** 366
[41] Romanov A E, Rozhkov M A and Kolesnikova A L 2018 *Lett. Mater.* **8** 384
[42] Barani E, Korznikova E A, Chetverikov A P, Zhou K and Dmitriev S V 2017 *Phys. Lett.* A **381** 3553
[43] Shcherbinin S A, Zhou K, Dmitriev S V, Korznikova E A, Davletshin A R and Kistanov A A 2020 *J. Phys. Chem.* C **124** 10235
[44] Kistanov A A, Khadiullin S K, Dmitriev S V, Korznikova E A 2019 *Chem. Phys. Lett.* **728**, 53
[45] Babicheva R I, Dahanayaka M, Liu B, Korznikova E A, Dmitriev S V, Wu M S and Zhou K 2020 *Mater. Sci. Eng.* B **259** 114569
[46] Kistanov A A, Khadiullin S K, Dmitriev S V and Korznikova E A 2019 *Chem. Phys. Chem.* **20** 575